Journal of Computer Science

Original Research Paper

IAFIR Optimization against NOMA Competitors: A Comprehensive Analysis on Energy-Efficient Non-Orthogonal Multiple Access

S. Pavithra and S. Chitra

Department of Electronics and Communication Engineering, Rajalakshmi Engineering College, Tamil Nadu, Chennai, India

Article history
Received: 21-12-2023
Revised: 26-03-2024
Accepted: 01-04-2024

Corresponding Author:
S. Pavithra
Department of Electronics and Communication Engineering, Rajalakshmi Engineering College, Tamil Nadu, Chennai, India
E-mail: pavithra.s@rajalakshmi.edu.in

Abstract: The ever-growing demands of next-generation wireless networks necessitate the exploration of innovative technologies to enhance spectral efficiency, user experience and network performance. Non-Orthogonal Multiple Access (NOMA) has emerged as a promising candidate, offering the potential for increased capacity and improved system reliability. NOMA allows multiple users to share the same time-frequency resource, breaking away from traditional orthogonal access methods. In NOMA, users are distinguished by different power levels, enabling simultaneous transmission and reception. This novel approach presents advantages in scenarios with a high density of connected devices, such as urban environments and Internet of Things (IoT) deployments, contributing to enhanced spectral efficiency. However, NOMA is not without limitations. One key challenge lies in the complexity of managing interference among users sharing the same resource, particularly as the number of users increases. Ensuring fairness and maintaining a balance in user quality of service becomes a critical concern. Efficient algorithms and schemes, such as the Interference Adaptive Fusion with Iterative Rejection (IAFIR), aim to address these limitations and enhance NOMA performance. The study focuses on the IAFIR scheme, a novel approach designed to mitigate interference and enhance the quality of service in NOMA scenarios. To comprehensively assess the effectiveness of IAFIR and its impact on next-generation wireless networks, a comparative analysis against other well-established NOMA techniques, including Iterative Interference Cancellation (IIC) and Interference Rejection Combining (IRC), is conducted. By understanding their performance characteristics and their applicability to various wireless network scenarios, the goal is to guide the development and deployment of more efficient and reliable next-generation wireless networks. The research lays the groundwork for potential extensions, particularly in the context of multiuser scenarios, where the performance of IAFIR can be evaluated in more complex environments.

Keywords: Conventional NOMA, Iterative Interference Cancellation (IIC), Interference Rejection Combining (IRC), Interference Adaptive Fusion with Iterative Rejection (IAFIR), Next-Generation Technology

Introduction

The ongoing evolution of NOMA promises to increase some advantages, further transforming wireless communication by addressing the increasing demands for high data rates, superior user experiences and more efficient network management. This, in turn, aligns with the ever-expanding ecosystem of connected devices and applications, shaping the wireless communication landscape in a profound and dynamic manner (Pavithra and Chitra, 2023). Interference in NOMA is a significant concern arising from the simultaneous transmission of multiple users on the same communication resources. It can manifest as both intra-user and inter-user interference, impacting the quality of service in NOMA-based networks (Chitra *et al*., 2015). Intra-user interference may occur when different data streams within a single user's transmission interfere with each other, particularly in

power-domain NOMA, where stronger users' signals may impede the reception of weaker users. On the other hand, inter-user interference results from the shared utilization of time or frequency resources among users, where signals from one user can interfere with signals from others, potentially degrading communication reliability. To mitigate these interference challenges, the novel approach of Interference Adaptive Fusion with Iterative Rejection (IAFIR) emerges as a promising solution. IAFIR employs adaptive interference rejection techniques and iterative signal processing, which work in concert to enhance the separation of user signals and minimize interference. This results in an improved quality of service, with users experiencing reduced interference, even in densely populated and congested network scenarios. IAFIR's adaptability to dynamic network conditions and its seamless integration with NOMA makes it a valuable innovation for addressing interference-related issues and optimizing the performance of NOMA in next-generation wireless networks. The increase in user traffic and the production of smart devices in recent years can only be aptly characterized as both exponential and phenomenal. The developments, coupled with the promises offered by 5G and beyond (CISCO, 2023) underscore the fact that merely optimizing bandwidth utilization will no longer suffice. This demands a comprehensive overhaul and enhancement of network infrastructure.

The rapid proliferation of wireless communication networks in recent years has brought about a surge in the demand for extraordinary data rates, reduced latency and seamless connectivity. This exponential growth, coupled with the increasing diversity of devices and applications, presents tough challenges to next-generation wireless networks (Qin *et al*., 2018). NOMA technology has emerged as a promising solution to address these challenges by enhancing spectral efficiency and system reliability. NOMA allows multiple users to share the same resources within a cell, effectively non-orthogonal in terms of time, frequency, or code domain, resulting in increased capacity and improved network performance (Jehan and Zeeshan, 2022).

The evolution of NOMA has produced notable advantages in the realm of wireless communication until 2023 (Chai *et al*., 2023; Zhu *et al*., 2023). These advantages have been instrumental in reshaping the landscape of mobile networks and services, bearing considerable significance for research and industry alike.

Spectral efficiency: It is the number of message bits per subcarrier. NOMA has a spectral efficiency of 1.6 at € =10-3 (Choi *et al*., 2023).

Enhanced throughput: Achieves an acceptable fairness rate while maximizing throughput by 9% (Mai *et al*., 2021).

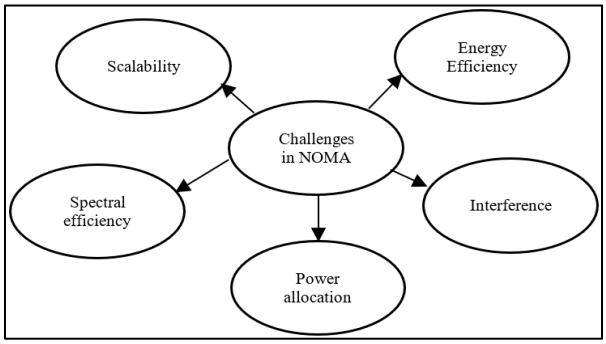

Fig 1: Challenges in NOMA

Table 1: List of abbreviations

Abbreviation	Definition
NOMA	Non-orthogonal multiple access
IIC	Iterative interference cancellation
IRC	Interference rejection combining
IAFIR	Interference adaptive fusion with iterative rejection
SIC	Successive interference cancellation
WHT	Walsh-hadamard transform
HetNet	Heterogeneous networks
FTPA	Fractional transmission power allocation
OFDM	Orthogonal frequency division multiplexing
CSI	Channel state information
DFT	Discrete fourier transform
IDFT	Inverse discrete fourier transform

Energy efficiency: The NOMA HetNet with the FTPA power allocation scheme exhibits a 27% higher energy efficiency compared to the OFDM HetNet with the Equal power (EQ) allocation scheme in the presence of imperfect channel CSI (Chen *et al*., 2021).

Quality of Service (QoS): NOMA's consistent quality of service assures users of reliable and high-quality connectivity, even during periods of peak network utilization (Pischella *et al*., 2020).

Despite hav`ing numerous advantages, NOMA still faces a few challenges that need to be addressed (Mohsan *et al*., 2023). Some of these challenges include energy efficiency, interference, power allocation, spectral efficiency and scalability Fig. 1. Table 1 shows the list of abbreviations used in the context of the research work.

In October, Chauhan and Jaiswal, (2023), introduced a novel PD-NOMA system, termed Multidimensional signal space NOMA (MD-NOMA), aimed at alleviating the abrupt degradation in performance metrics like Average Sum-Rate (ASR), outage performance and ϵ-outage capacity. The authors also demonstrated that MD-NOMA remains robust even with higher Modulation orders (M), in stark contrast to all other systems, which experience significant performance degradation as M increases.

In the study by Abd-Alaziz *et al*. (2023), a structured coding scheme has been developed. Essentially, this proposed technique centers on establishing a connection between the transmitted data waveforms of the users and subsequently employing this connection in the decoding process at the receiving end. The coding and decoding techniques introduced in their work exhibit superior performance and reduced complexity when compared to conventional uncoded NOMA.

Hama and Ochiai (2023) introduced a power-efficient Non-Orthogonal Multiple Access (NOMA) scheme tailored for Internet of Things (IoT) and Device-to-Device (D2D) communications. However, a significant hurdle remains in the form of the Peak Average Power Ratio (PAPR). To overcome this challenge, the authors proposed the integration of the Time-Frequency domain NOMA (TF-NOMA), wherein OFDM and DFT-spread OFDM (DFT-s-OFDM) are overlaid across the time frequency domain. Their experiments demonstrated that TF-NOMA outperforms conventional PD-NOMA, showcasing a noteworthy improvement in error rate performance.

Issa *et al*. (2023) introduced a data-driven uplink NOMA model with meta-learning assistance designed to minimize channel estimation overhead. The findings indicate that their meta-SICNet surpasses classical SIC and conventional SICNet, achieving a lower symbol error rate while using fewer pilots.

Khan *et al*. (2023) addressed issues associated with Device-to-Device (D2D) communication. The D2D process introduces cross-channel and co-channel interference for cellular and other D2D users, presenting a considerable challenge in spectrum allocation. To tackle this obstacle, the researchers integrated Nonorthogonal Multiple Access (NOMA) with the D2D Groups (DGs). Their objective was to maximize the overall network's sum throughput while preserving the Signal-to-Interference Noise Ratio (SINR) for both cellular and D2D users.

He *et al*. (2023) introduced an innovative signal-processing framework for massive MIMO-NOMA data transmission. The proposed approach utilizes Group Level Successive Interference Cancellation (GLSIC), wherein users are grouped based on their distances from the Base Station (BS). NOMA is then implemented among different groups using GLSIC to diminish inter-group interference. Theoretical analysis and simulation results demonstrate that, under identical conditions, the GLSIC-based system achieves a higher uplink rate compared to the existing cluster-based MIMO-NOMA system with user-level SIC.

Tabeshnezhad *et al*. (2023) explored an uplink power-domain NOMA system enhanced by a Reconfigurable Intelligent Surface (RIS) in the presence of a jammer seeking to maximize interference on the Base Station (BS) uplink receiver. Numerical results indicate that the RIS significantly reduces the per-user required transmit power in an interference-limited scenario.

Also, (Rito and Li, 2023) integrated two techniques, combining RIS with NOMA in an approach termed RIS-assisted NOMA. They introduced an interference cancellation scheme where a group of phase shift elements is assigned to mitigate interference to users not currently supported. Additionally, they proposed an interference-alignment scheme when the RIS is supporting all NOMA users.

Soni *et al*. (2023) investigated underlay opportunistic communication in a cognitive radio system, employing an effective blend of Opportunistic Interference Alignment (OIA) and NOMA. OIA, a well-known precoding technique in Multiple-Input Multiple-Output (MIMO) systems, utilizes interference alignment over spatial dimensions to enhance the rate of cognitive users. The proposed OIA-based MIMO-NOMA system achieves an improved sum rate for cognitive users compared to the conventional OIA-based MIMO-OMA system.

Hu *et al*. (2023) proposed a novel framework integrating power domain NOMA and multi-antenna technology with a group-based Successive Interference Cancellation (SIC). The proposed scheme outperforms conventional Orthogonal Multiple Access (OMA) and existing cluster-based NOMA schemes in terms of total power consumption.

Budhiraj *et al*. (2022) introduced the "interference reduction scheme for Device-to-Device (D2D) mobile groups using uplink NOMA (ISHU)" with the aim of improving network throughput. Simulation results demonstrated that ISHU achieves notably superior throughput, surpassing existing uplink conventional NOMA and OFDMA schemes by 3.846 and 26.92%, respectively.

Chitra *et al*. (2020) proposed correlative coding between binary symbols modulated on adjacent subcarriers, aiming to reduce Inter-Carrier Interference (ICI) without incurring any spectral loss. Simulation results demonstrate that the proposed PRCC method yields superior Carrier-to-Interference Ratio (CIR) and Bit Error Rate (BER) performance compared to the conventional Conjugate Cancellation (CC) technique.

Existing Work

NOMA receives praise for revolutionizing wireless communication by allowing multiple users to share resources simultaneously. However, implementing NOMA encounters challenges, especially interference issues in conventional NOMA. This interference notably affects network performance, particularly in high-density scenarios where users compete for limited resources. Addressing these challenges is crucial for optimizing NOMA's efficiency in wireless communication systems.

Basic NOMA

In wireless communication, multiple devices communicate with a central hub or base station. These devices often have limited power and efficient use of the available spectrum is crucial. NOMA can be applied in wireless networks to enhance spectral efficiency by allowing multiple devices to share the same time-frequency resource (Ghafoor *et al*., 2022):

$$y = h1\sqrt{P1}\,s1 + \sqrt{P2}\,s2 + n \quad (1)$$

- h_1h_1 and h_2h^2 represent the channel gains for the signals transmitted
- $P1$ and $P2$ are the power levels allocated to the signals
- $s1$ and $s2$ are the transmitted signals
- n is the additive white Gaussian noise

Ideal SIC Process

Decoding user 2's signal:

$$\hat{s}_2 = \frac{h_2^*}{|h_2|}\sqrt{P_2}s_2 + \frac{h_1}{|h_2|}\sqrt{P_1}s_1 + \hat{n}_2 \quad (2)$$

where:
h_2^* = The complex conjugate of h_2
$|\cdot|$ = Denotes the absolute value
$\hat{n}_2$ = The effective noise after decoding user 2's signal

Removing Interference from User 2's Signal

The interference from user 2's signal is subtracted from the received signal:

$$y^{\sim 1} = y - h_2\sqrt{(P2)}\,s^2 \quad (3)$$

The newly received signal is used for decoding user 1's signal.

Decoding user 1's signal:

$$\hat{s}_1 = \frac{h_1^*}{|h_1|}\sqrt{P_1}s_1 + \hat{n}_1 \quad (4)$$

where:
h_1^* = The complex conjugate oh h_1
$\hat{n}_1$ = The effective noise after decoding both users 2 and 1

Non-Ideal SIC Process

Decoding user 2's signal:

$$\hat{s}_2 = \beta\frac{h_2^*}{|h_2|}\sqrt{P_2}s_2 + \frac{h_1}{|h_2|}\sqrt{P_1}s_1 + \hat{n}_2 \quad (5)$$

- β is a factor accounting for non-ideal conditions
- h_2^* is the complex conjugate of $h2$
- $|\cdot|$ denotes the absolute value
- $\hat{n}_2$ is the effective noise after decoding User 2's signal

Interference Residue in Non-Ideal SIC

The interference residue, ϵ, remains due to non ideal conditions:

$$\epsilon = h_2\sqrt{P_2}s_2 \quad (6)$$

This interference residue impacts the subsequent decoding process.

Decoding User 1's Signal with Residual Interference

$$\hat{s}_1 = \frac{h_1^*}{|h_1|}\sqrt{P_1}s_1 + \epsilon + \hat{n}_1 \quad (7)$$

where:
h_1^* = The complex conjugate oh h_1
$\hat{n}_1$ = The effective noise after decoding both users 2 and 1

Iterative Interference Cancellation (IIC) was initially introduced to address interference challenges and maximize the potential of NOMA. This innovative approach applies iterative signal processing to separate and decode user signals while canceling interference through successive iterations. Although IIC enhances signal separation and reduces interference, it encounters limitations such as the requirement for prior channel knowledge, which hampers real-time implementation and poses challenges for massive connectivity (Chitra *et al*., 2020). The computational complexity raises concerns about practical deployment. To overcome these limitations, researchers have developed solutions like IRC, representing ongoing efforts to refine interference mitigation techniques in NOMA networks.

Interference Rejection Combining (IRC) further refines interference mitigation within NOMA systems. IRC introduces a combining method that not only enhances signal separation but also reduces computational complexity, rendering it suitable for real-world deployment (Srinivasan *et al*., 2021). Particularly vital in dynamic channel conditions, IRC enhances signal separation and interference rejection, thereby improving the quality of service in NOMA networks. It excels notably in scenarios with high user density and interference-prone environments, minimizing transmission errors and ensuring reliable communication. The transition from IIC to IRC marks a significant advancement in tackling the interference challenges inherent in conventional NOMA, paving the way for innovative solutions like IAFIR. These developments underscore the continuous efforts aimed at enhancing NOMA's efficiency and reliability in modern wireless networks, with IAFIR showing promise for optimized performance across diverse network scenarios.

The existing algorithms, Iterative Interference Cancellation (IIC) and Interference Rejection Combining (IRC) face several limitations that hinder their performance in wireless communication systems (Chitra *et al*., 2023). Both IIC and IRC rely on fixed power allocation schemes, resulting in suboptimal performance and inefficient resource usage. Moreover, these algorithms lack dynamic adaptation to changing channel conditions, impeding their ability to effectively mitigate interference. Consequently, both algorithms demonstrate reduced system capacity and performance, particularly in high-interference scenarios. Furthermore, the fixed allocation schemes worsen interference issues in crowded environments, compromising communication reliability.

Various simulations were conducted on existing algorithms and a few outputs are illustrated in Figs 2-4. In contrast, the proposed Interference Adaptive Fusion with Iterative Rejection (IAFIR) algorithm addresses these drawbacks by introducing dynamic power allocation and employing advanced interference mitigation techniques such as the Walsh-Hadamard Transform and cyclic prefix. With its adaptive filtering mechanisms, IAFIR ensures robust performance across varying channel conditions, providing a comprehensive solution to the limitations of existing algorithms and paving the way for enhanced wireless communication capabilities (Hama and Ochiai, 2023).

Proposed Work

Figure 5 depicts the model of the proposed IAFIR structure. This model exhibits significant enhancement compared to the conventional NOMA system by incorporating the Walsh-Hadamard transform at both the transmitter and receiver end. The utilization of Walsh codes assists in reducing interference among users, as each user's signal is spread using a distinct code. Furthermore, the inclusion of the cyclic prefix aids in mitigating the impacts of multipath fading by offering a guard interval between symbols.

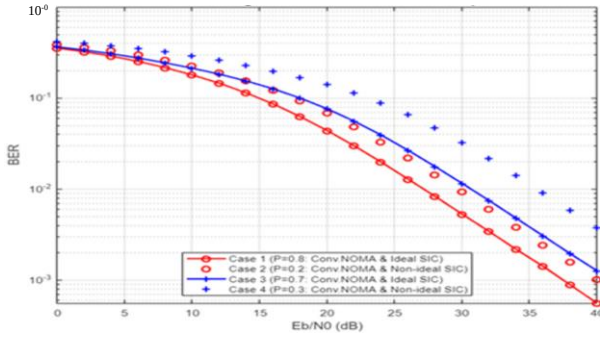

Fig. 2: Performance analysis of BER of NOMA using QPSK modulation with various power allocation

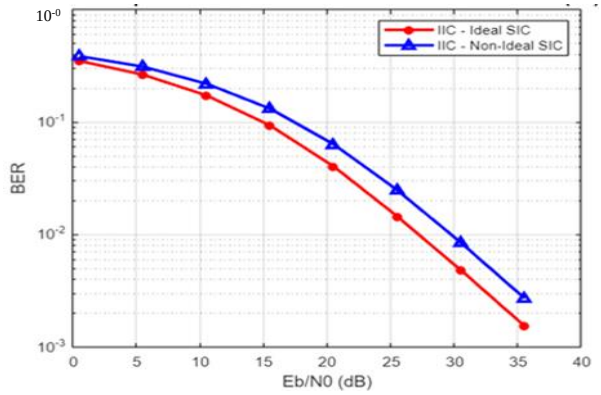

Fig. 3: Performance analysis of BER of IIC using QPSK modulation

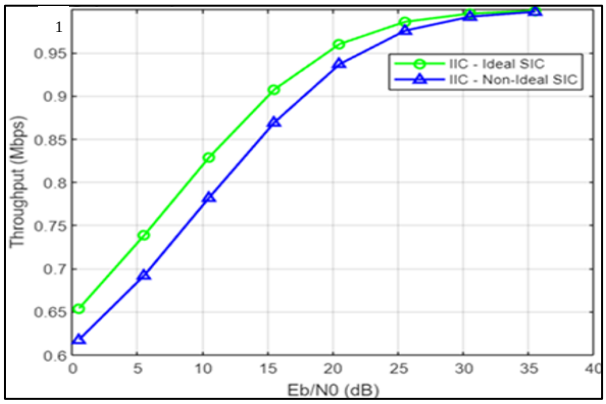

Fig. 4: Performance analysis of throughput of IIC using QPSK modulation

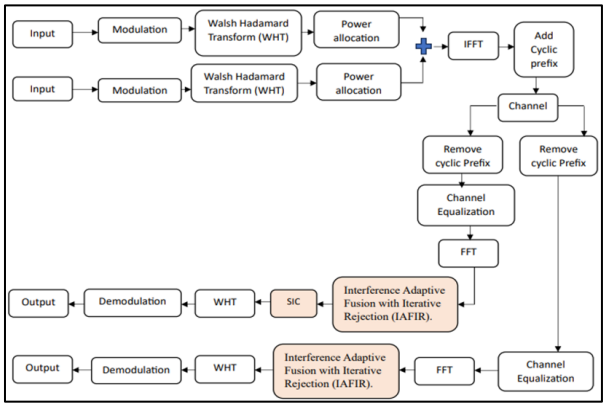

Fig. 5: The proposed IAFIR structure

During the initialization phase, various system parameters are defined to establish the wireless communication system. This involves specifying parameters such as the Number of symbols (N), distances between users (d1 and 2) and power allocation factors (a1 and 2) for users 1 and 2 (considering only 2 users for simplicity, but can be extended to multiple users), path

loss exponent (eta), Transmit Power (Pt), Bandwidth (BW), Noise power (No) and initial Signal-to-Noise Ratio (SNR) values in decibels. Following this, random modulated symbols are generated for both users 1 and 2, representing the information to be transmitted. Subsequently, the Walsh-Hadamard Transform (WHT) matrix is applied to these modulated symbols, serving to spread and encode the information.

$$xk = sk * wk$$

xk = spread symbol for the k^{-th} user,
sk = original modulated symbol and
wk= k^{-th} row of the Walsh-Hadamard matrix

Following this, the power allocation factors are introduced

Transmit Power Range (*Pt*)

The variable '*Pt*' represents a range of transmit powers in dBm. This range is specified as 0.1:5:40, generating a sequence of transmit power values from 0.1-40 dBm with a step size of 5 dBm.

Linear Scale Power (*pt*)

The linear scale power values, denoted as pt, are calculated using the formula.

$$\mathrm{Pt} = (10^{-3}) * 10^{(\mathrm{Pt}/10)}$$

Power Allocation Factors (*a1 and 2*)

The power allocation factors a1 and 2 respectively. These factors determine the proportion of total power allocated to each user.

Superposition Coding with Power Allocation

The next step involves superposition coding with power allocation which is calculated for both users based on the channel conditions and power allocation factors (a1 and 2). Superposition coding is applied to user signals (x1 and 2) using the transmit power values (pt) and power allocation factors (a1 and 2) for instance:

$$x\_ideal = \sqrt{pt(u) * (\sqrt{a1} * x1 + \sqrt{a2} * x2)}$$

The transmitted power for both users is then adaptively adjusted to maximize their SINR, effectively managing interference and ensuring that each user's signal is received with minimal interference from the other user. Proceeding to the transmission phase, the adapted signals from users 1 and 2 are combined and prepared for transmission. The combined signal undergoes Inverse Fast Fourier Transform (IFFT) as part of the signal processing:

$$x(t) = \frac{1}{\sqrt{N}} \sum_{k=0}^{N-1} X(k) e^{j2\pi \frac{kt}{T}}$$

To mitigate the effects of multipath fading in the channel, a cyclic prefix is added to the signal in the subsequent step. In this example, the length of the cyclic prefix is assumed to be 1:

$$xCP(t) = [Cyclic\ Prefix] + x(t)$$

These sequential steps collectively form the process of initializing, generating, transforming, modeling, adapting, transmitting and adding a cyclic prefix in a wireless communication system.

Receiver Processing

Upon receiving the transmitted signal, the first step involves separating it into two distinct parts designated for users 1 and 2, respectively. Following this, the cyclic prefix is removed from both signals to prepare them for further processing. Equalization is then applied to both received signals as a compensatory measure against channel effects, aiming to accurately recover the originally transmitted symbols. The signals are subsequently transformed back into the frequency domain through the Fast Fourier Transform (FFT). To mitigate interference, Interference Rejection Combining (IRC) is applied to both signals, reducing interference caused by the other user's signal and facilitating improved signal recovery. Additionally, Successive Interference Cancellation (SIC) is employed, utilizing an iterative decoding technique to further diminish interference from other users. The next step involves demodulating the signals and extracting the final decoded information bits for both users 1 and 2. To assess the quality of the received information, the Bit Error Rate (BER) is calculated for both users by comparing the decoded bits with the originally transmitted bits. To obtain more reliable results, the entire process is reiterated multiple times, as specified by the number of iterations and the BER results are averaged. This comprehensive sequence of steps encompasses separation, preprocessing, interference reduction, demodulation and BER calculation processes, providing a systematic approach to evaluating and improving the accuracy of information recovery in a wireless communication system.

Innovations and Improvements Made to IAFIR

Dynamic power allocation: IAFIR dynamically adjusts transmit power based on real-time channel conditions, optimizing spectral efficiency and minimizing interference.

Superposition coding optimization: Utilizes superposition coding to optimize transmit power values, enhancing data throughput while maintaining signal integrity.

Interference mitigation techniques: Incorporates advanced interference rejection combining and successive interference cancellation methods to minimize the impact of interference on signal reception.

Cyclic prefix implementation: Adds cyclic prefixes to transmitted signals to mitigate multipath fading effects, ensuring robust signal recovery at the receiver.

Adaptive equalization and demodulation: Employs adaptive equalization algorithms to compensate for channel distortions, enhancing the accuracy of demodulation and reducing error rates in data transmission.

Materials and Methods

Simulation Environment

The simulation of the proposed IAFIR structure was carried out using MATLAB. MATLAB provides an extensive suite of tools for modelling, simulation and analysis of wireless communication systems. The parameters and configurations used in the simulation adhered to the 3rd Generation Partnership Project (3GPP) standards to ensure relevance and applicability to real-world scenarios.

System Parameters

The key system parameters used in the simulation are listed below:

- Number of symbols (N): 1024
- User distances (d1 and d2): 50 meters and 100 meters
- Power allocation factors (a1 and a2): 0.7 and 0.3
- Path loss exponent (eta): 3.5
- Transmit Power (Pt): 0.1 to 40 dBm
- Bandwidth (BW): 20 MHz
- Noise Power (No): -174 dBm/Hz
- Initial SNR values: 0-20 dB

Modulation Schemes

Different modulation schemes were used to evaluate the performance of the proposed system under varying conditions. The modulation schemes included:

- Quadrature Phase Shift Keying (QPSK)
- 16-Quadrature Amplitude Modulation (16-QAM)
- 64-Quadrature Amplitude Modulation (64-QAM)
- 256-Quadrature Amplitude Modulation (256-QAM)

Walsh-Hadamard Transform

The Walsh-Hadamard Transform (WHT) was utilized for spreading and encoding the signals. This transform helps in reducing interference among users by assigning distinct orthogonal codes to each user's signal.

Power Allocation and Superposition Coding

Power allocation factors (a1 and 2) were determined based on the channel conditions and total power constraints. Superposition coding was applied to combine the signals of users 1 and 2 using the calculated power allocation factors and transmit power values. This process ensures that the signals are transmitted with appropriate power levels to maximize Signal-to-Interference-plus-Noise Ratio (SINR) and minimize interference.

Channel Model

The wireless channel was modeled to include multipath fading effects using a Rayleigh fading channel model. A cyclic prefix was added to mitigate the effects of inter-symbol interference caused by multipath fading.

Receiver Processing

At the receiver end, the following steps were implemented.

Signal separation: The received signal was separated into individual user signals.

Cyclic prefix removal: The cyclic prefix was removed to prepare the signals for further processing.

Equalization: Channel equalization was performed to compensate for the distortions introduced by the wireless channel.

FFT processing: The signals were transformed back into the frequency domain using FFT.

Interference Rejection Combining (IRC): IRC was applied to reduce interference from other users.

Successive Interference Cancellation (SIC): SIC was employed to iteratively decode and further reduce interference

Demodulation: The signals were demodulated to recover the original information bits.

Bit error rate calculation: The BER was calculated by comparing the decoded bits with the originally transmitted bits.

Performance Metrics

The performance of the proposed IAFIR structure was evaluated based on several key metrics:

- Bit Error Rate (BER): Measured to assess the accuracy of the received information
- Throughput: Evaluated to determine the data transmission efficiency
- Computational complexity: Analyzed to understand the processing requirements of the proposed method

- Carrier-to-Interference Power Ratio (CIR): Measured to evaluate the effectiveness of interference mitigation techniques

Results and Discussion

This section presents the simulation results of the proposed work, comparing it with conventional NOMA (discussed in the section 'existing work' along with Figs. 2-4) under both ideal and non-ideal conditions. The simulation parameters in this study adhere to the specifications outlined by the 3rd Generation Partnership Project (3GPP), as detailed in Table 2. While the primary objective of this research is to enhance the performance of IAFIR, any power allocation scheme could be utilized. However, for the sake of simplicity, we have adopted fixed power allocation for both users, with the total power set to 1.

The simulation outcomes for the IAFIR approach are compared with conventional NOMA, IIC and IRC under both ideal and non-ideal conditions. The findings are analyzed in terms of Bit Error Rate (BER), Throughput, Computational Complexity and Carrier-to-Interference Power Ratio (CIR) across various modulation schemes.

Additional detailed parameters for both ideal and non ideal conditions in the simulation are provided in Table 3.

Bit Error Rate: Ideal Conditions

Figures 6-9 illustrate the Bit Error Rate (BER) performance of both ideal and non-ideal Successive Interference Cancellation (SIC). Figures 6 and 7 represent the ideal SIC for QPSK and 8 QAM, while Figs. 8-9 depict the non-ideal SIC for QPSK and 8 QAM. Higher-order modulation was utilized for simulation purposes. Figures 6-7, the BER value for conventional NOMA with ideal SIC at 5 dB is close to 100, which is undesirable. In contrast, for IAFIR, the BER is close to 10-1. The performance gain for both ideal and non-ideal cases remain almost the same, i.e., 5-10 dB. There is a significant improvement in receiver performance in terms of BER.

Table 2: Simulation parameters

Bandwidth	1.4 MHz
Wireless access method	OFDM
Subcarrier spacing	15 KHz
Subcarrier count	600
FFT length	2048
Frame duration	0.5 ms
Doppler spread	2.0 Hz
Data modulation	QPSK, 8 QAM
Timing alignment	Perfect
Time domain synchronization	Ideal

Table 3: Additional simulation parameters used for simulation of ideal and non-ideal SIC

Distances of users (m)	d_1=1000 and d_2 = 500
Power allocation factors for users	a_1 = 0.9 and a_2 = 0.1
Path loss exponent	$\eta = 4$
Rayleigh fading coefficients for both users	$h_1 = \sqrt{\frac{1}{d1\eta}}$ (randn (1, N) + i * randn (1, N))/ $\sqrt{2}$ $h_2 = \sqrt{\frac{1}{d2\eta}}$ (randn (1, N) + i * randn (1, N))/ $\sqrt{2}$
Squared magnitudes of the fading coefficients-channel gain	$g_1 = \|h1\|^2$ and $g_2 = \|h_2\|^2$
Transmit power in dBm	P_t = 0.1: 5: 40
Transmit power in linear scale	$p_t = (10^{-3}) * 10 (Pt/10)$
System bandwidth	BW =106 Hz
Noise power in dBm	$N_o = -174+10*\log_{10}(BW)$
Noise power in linear scale	$N_o = (10^{-3}) * 10 (N_o/10)$
Signal-to-Noise Ratio (SNR) in dB	$SNR = P_t-10*\log_{10}(BW) +60$

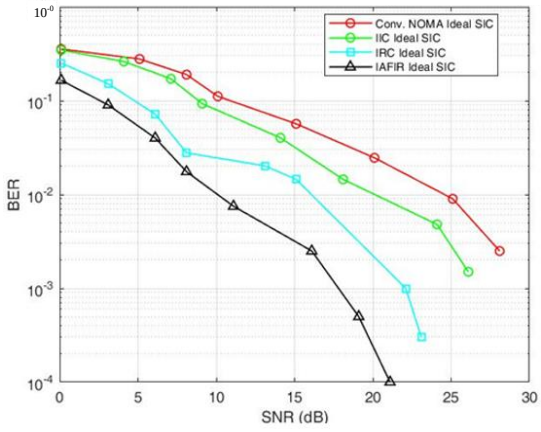

Fig. 6: BER performance analysis-ideal-QPSK

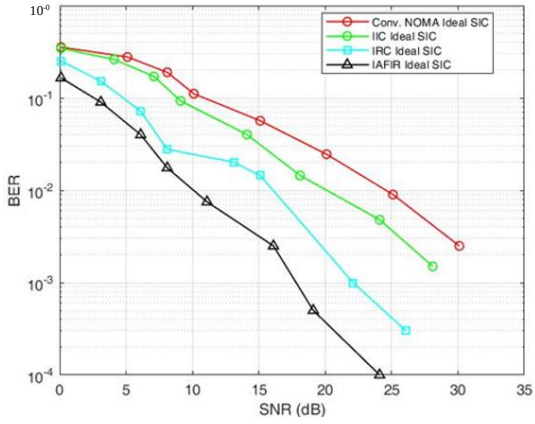

Fig. 7: BER performance analysis-ideal-8 QAM

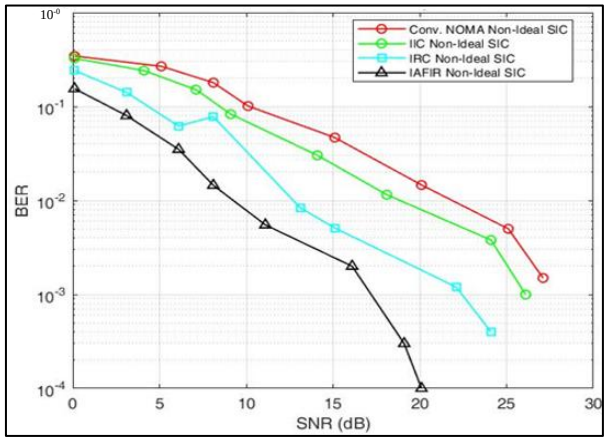

Fig. 8: BER performance analysis-non-ideal-QPSK

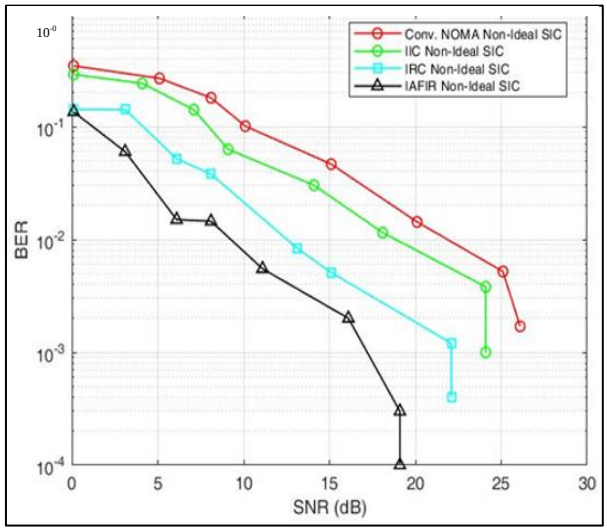

Fig. 9: BER performance analysis-non-ideal-8QAM

Bit Error Rate-Non-Ideal Condition

Table 4, the Ideal SIC scenario of IAFIR consistently demonstrates superior error performance compared to its non-ideal SIC counterpart, highlighting the effectiveness of interference rejection and decoding capabilities in the ideal setting. Similarly, the Ideal SIC scenarios of IRC and IIC show improved BER values compared to their non-ideal counterparts, emphasizing the significance of optimal interference handling for these methods. The BER comparison also positions IAFIR favorably against conv. NOMA, suggests that, under the simulated conditions, IAFIR excels in minimizing bit errors. The investigation highlights a noteworthy performance gain of approximately 5-10 dB in the Signal-to-Noise Ratio (SNR) for different BER values under both perfect and imperfect SIC conditions compared to conventional NOMA. The utilization of Walsh-Hadamard Transform (WHT) significantly reduces BER, enhancing overall performance in IAFIR.

Throughput-Ideal

$T= (1-BER) * B* \log_2 (Q)$:

- B- bandwidth
- Q-modulation order

Figures 10-13 depict the throughput performance of both ideal and non-ideal Successive Interference Cancellation (SIC). Remarkably, IAFIR exhibits superior performance compared to conventional methods. For instance, in Fig. 10, there is a 0.36 Mbps increase at 5 dB SNR for ideal QPSK and a 0.22 Mbps increase for ideal 8 QAM. Similarly, in the case of non-ideal SIC Figs. 12-13, there is approximately a 0.5 Mbps increase for QPSK and a 0.7 Mbps increase for 8 QAM at 5 dB SNR.

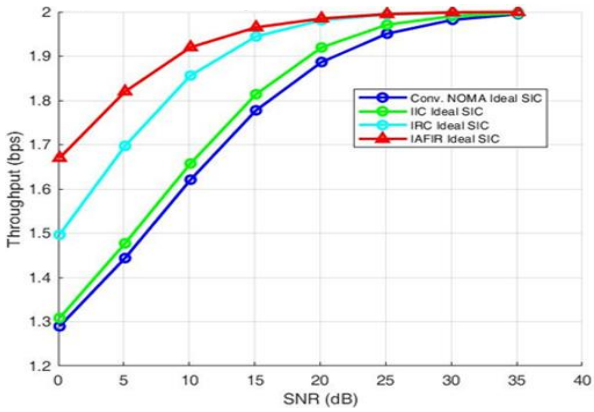

Fig. 10: Throughput-ideal-QPSK

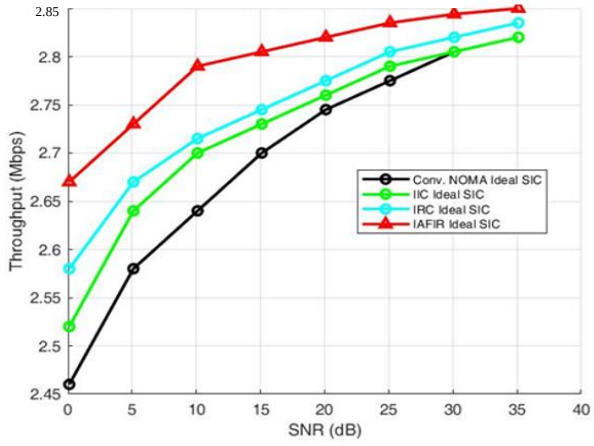

Fig. 11: Throughput-ideal-8 QAM

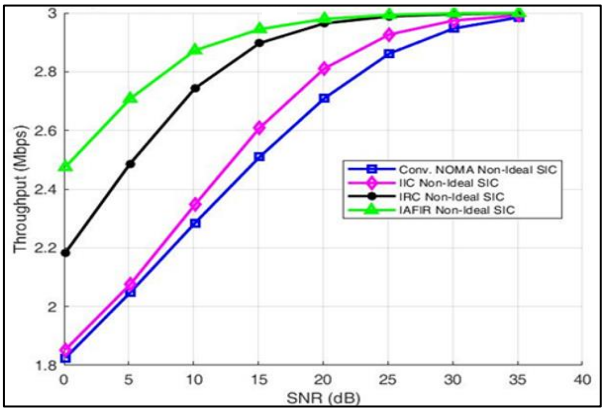

Fig. 12: Throughput-non-idel-QPSK

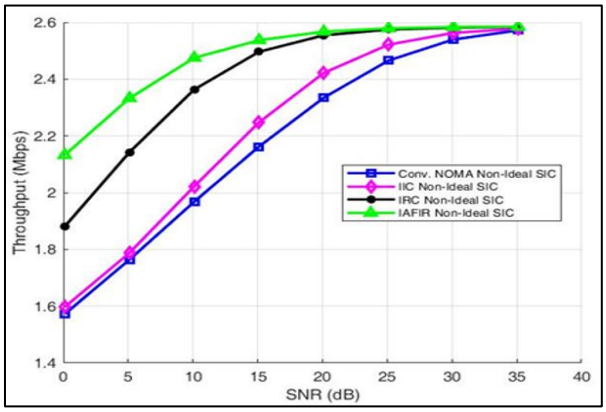

Fig. 13: Throughput-non-ideal-8 QAM

Table 4: Performance analysis of bit error rate for various Signal-to-Noise Ratios (SNRs)- QPSK

SNR (dB)	Conv. NOMA ideal SIC (Mbps)	Conv. NOMA non-ideal SIC (Mbps)	IIC ideal SIC (Mbps)	IIC non-ideal SIC (Mbps)	IRC ideal SIC (Mbps)	IRC non-ideal SIC (Mbps)	IAFIR ideal SIC (Mbps)	IAFIR non-ideal SIC (Mbps)
10	0.355	0.392	0.3458	0.3823	0.2517	0.2724	0.1764	0.1642
15	0.278	0.318	0.2615	0.3083	0.1514	0.1711	0.104	0.0915
20	0.019	0.239	0.1712	0.2177	0.0719	0.0856	0.006	0.0476
25	0.111	0.163	0.0093	0.1304	0.0278	0.0342	0.0333	0.0212
30	0.057	0.097	0.0402	0.0063	0.0094	0.0118	0.0172	0.0005
35	0.025	0.046	0.0145	0.0245	0.0031	0.0039	0.0074	0.0022
40	0.009	0.018	0.0048	0.0085	0.0001	0.0013	0.0014	0.0001

Table 5: Performance analysis of throughput for various Signal-to-Noise Ratios (SNRs)-QPSK

SNR (dB)	Conv. NOMA Ideal SIC (Mbps)	Conv. NOMA non-ideal SIC (Mbps)	IIC ideal SIC (Mbps)	IIC non-ideal SIC (Mbps)	IRC ideal SIC (Mbps)	IRC non-ideal SIC (Mbps)	IAFIR ideal SIC (Mbps)	IAFIR non-ideal SIC (Mbps)
10	0.6448	0.6083	0.6542	0.6177	0.7483	0.7276	0.8358	0.7376
15	0.7219	0.6825	0.7385	0.6917	0.8486	0.8289	0.9085	0.829
20	0.8104	0.7614	0.8288	0.7823	0.9281	0.9144	0.9524	0.84
25	0.888	0.8366	0.907	0.8696	0.9722	0.9658	0.9788	0.8667
30	0.9433	0.9032	0.9598	0.937	0.9906	0.9882	0.995	0.8828
35	0.9745	0.9539	0.9855	0.9755	0.9969	0.9961	0.9978	0.8926
40	0.991	0.9825	0.9952	0.9915	0.999	0.9987	0.999	0.8986

Throughput-Non-Ideal

Upon analyzing the throughput comparison in Table 5, it becomes evident that the IAFIR scheme consistently outperforms other multiple access methods, including IIC, IRC and Conv. NOMA, across various SNR levels. At an SNR of 10 dB, IAFIR achieves a throughput of 0.8236 in ideal conditions, surpassing the corresponding values for IIC (0.6542), IRC (0.7483) and Conv. NOMA (0.6448). In the non-ideal scenario at the same SNR, IAFIR maintains a superior throughput of 0.8358 compared to the competing methods. This trend persists across all SNR levels, indicating the consistent and superior performance of IAFIR. The adaptability of IAFIR in rejecting interference in fading channels enables it to achieve higher throughput even in challenging communication environments. The values in the table consistently demonstrate that IAFIR provides better communication efficiency, making it a robust and reliable choice for scenarios where interference rejection is critical for optimal system performance.

Fairness Index

The fairness index is computed from throughput, usually measured in bits per second (bps). To normalize

the throughput values for each user, divide the throughput of each user by the maximum throughput in the system. Normalization ensures that the fairness index remains independent of the absolute throughput values. One commonly used fairness index is Jain's fairness index, which is defined as:

$$Fairness\ Index = \frac{\left(\sum Throughput_i\right)^2}{N\sum\left(Throughput_i^2\right)}$$

The fairness index values offer valuable insights into the equitable distribution of resources among users in different scenarios. Across all three scenarios, NOMA, IIC, IRC and IAFIR demonstrate varying degrees of fairness. According to Fig. 14, IAFIR consistently outperforms its counterparts with the highest fairness index of 0.95, indicating superior resource allocation fairness compared to NOMA (0.8), IIC (0.9) and IRC (0.85). This trend persists in scenario 2 (Table 6), where IAFIR maintains its dominance with a fairness index of 0.9, surpassing NOMA, IIC and IRC. In the third scenario, IAFIR once again demonstrates its effectiveness by achieving the highest fairness index of 0.8. Consequently, the consistent superiority of IAFIR across all scenarios establishes it as the preferred choice for achieving equitable resource distribution, making it a compelling option in scenarios where fairness is a critical consideration.

Carrier to Interference Ratio (CIR)

Figures 15-16 demonstrate a significant improvement in Carrier-to-Interference power Ratio (CIR) performance. Specifically, there is a 4 dB increase between 5-10 dB SNR in QPSK and a 5 dB increase between 5-10 dB SNR in QAM.

Table 6: Fairness index analysis

NOMA	IIC	IRC	IAFIR
0.8	0.9	0.85	0.95
0.7	0.8	0.75	0.9
0.6	0.7	0.65	0.8

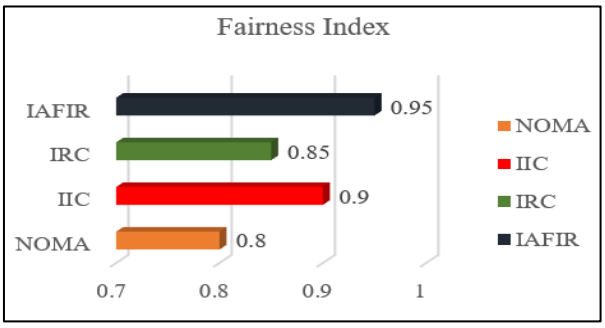

Fig. 14: Fairness index

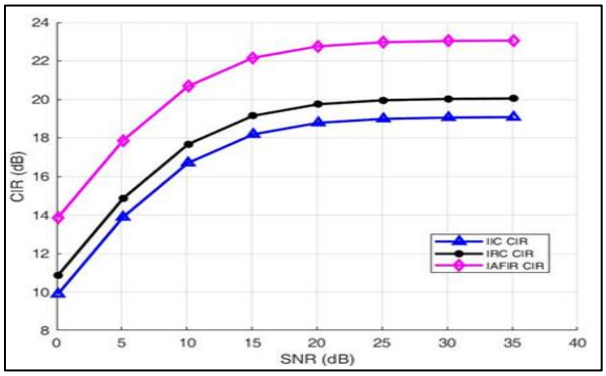

Fig. 15: Carrier to interference ratio-QPSK

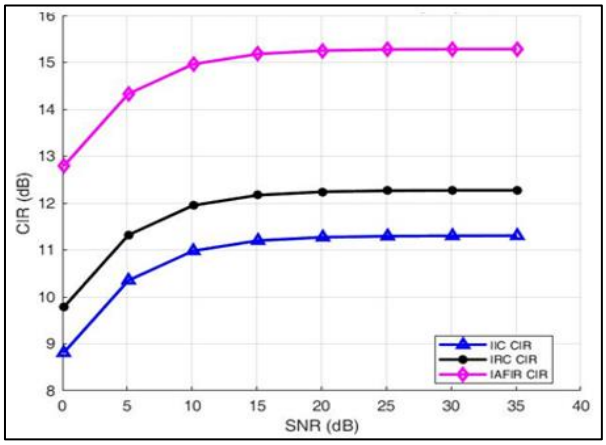

Fig. 16: Carrier to interference ratio-8 QAM

Table 7: Performance analysis of carrier-to-interference ratio for various Signal-to-Noise Ratios (SNRs)-QPSK

SNR (dB)	IIC	IRC	IAFIR
10	16.03	17.08	21.00
15	18.00	19.01	22.00
20	18.05	19.09	22.02
25	18.06	20.00	23.00
30	18.07	20.02	23.05
35	18.07	20.02	23.08
40	18.07	20.02	23.09

Table 8: Computation complexity analysis

	Transmitter	
Operation	NOMA	IAFIR
No. of complex multiplication	$L/_2 \log_2 (L)$	$L/2 \log_2 (L) +L$
No. of complex addition	$L \log_2 (L)$	$L \log_2 (L) +L$
Receiver		
Operation	NOMA	IAFIR
No. of complex multiplication	$L/2 \log_2 (L) +L$	$L/2 \log_2 (L) +L^2$
No. of complex addition	$L \log_2 (L)$	$L \log_2 (L) +L$

Computational Complexity

Table 7 provides carrier-to-interference ratio values for different scenarios (IIC, IRC, IAFIR) at various SNR levels (10, 15, 20, 25, 30, 35 and 40 dB) in the comparison table. A higher CIR indicates better system performance. Across all SNR levels, IAFIR consistently demonstrates a higher CIR compared to IIC and IRC. Notably, at lower SNR values (e.g., 10 and 15 dB), the difference in CIR between IAFIR and other schemes is significant. As SNR increases, the relative performance differences among IIC, IRC and IAFIR become more apparent, with IAFIR maintaining a clear advantage. Conversely, a lower CIR suggests that the interference is more prominent relative to the carrier signal, potentially leading to degraded signal quality and communication performance.

Table 8, the computational complexity analysis is explained using NOMA system, the IDFT operation is conducted at the transmitter. The computational complexity of the IDFT is well-known and can be expressed as O (N log N) using the Fast Fourier Transform (FFT) algorithm, where N represents the number of samples or subcarriers.

Similarly, in the IAFIR system, the IDFT operation is performed, but it is followed by an additional block of the Walsh-Hadamard Transform (WHT). The computational complexity of the WHT can be expressed as O (N) using efficient algorithms.

The computational complexity analysis offers insights into the efficiency of both conventional NOMA and the proposed IAFIR systems. In both systems, the essential operations involve the Inverse Discrete Fourier Transform (IDFT) at the transmitter and the Discrete Fourier Transform (DFT) at the receiver. However, the IAFIR system introduces an additional block of the Walsh-Hadamard Transform (WHT), which impacts the overall computational complexity.

Considering 'l' as the total number of subcarriers in the system, the required number of complex multiplications and additions at the transmitter and receiver for both NOMA and IAFIR are detailed in the analysis.

Concerning complex multiplications, NOMA demonstrates a logarithmic increase in complexity concerning 'l', while IAFIR exhibits a linear growth pattern. This suggests that as the number of subcarriers increases, NOMA tends to have lower computational complexity in terms of complex multiplications.

Conversely, regarding complex additions, NOMA showcases a linear increase in complexity with 'l', typically exceeding IAFIR in this aspect. As the number of subcarriers escalates, the complexity gap between NOMA and IAFIR becomes more apparent in terms of complex additions.

Overall, the analysis indicates that while NOMA may be more efficient concerning complex multiplications, especially with many subcarriers, IAFIR emerges as more efficient in the realm of complex additions. This underscores the trade-off between the two systems in terms of computational complexity and emphasizes the importance of considering specific system requirements and constraints when selecting between NOMA and IAFIR for practical implementations. From these complexities, we derive the following formulas:

$$NOMA: \mathrm{L} / 2 * log2(L)$$

(where L denotes the total number of subcarriers).

$$IAFIR: \mathrm{L} / 2 * log2(L) + L$$

Conclusion

The introduction of the IAFIR scheme in this research represents a significant advancement in NOMA systems, particularly in accommodating multiple users. By employing the Walsh-Hadamard transform at both transmitter and receiver ends, IAFIR effectively addresses interference issues, thereby enhancing spectral efficiency. Simulation analyses indicate substantial improvements in Bit Error Rate (BER) and throughput performance, especially in scenarios with low Signal-to-Noise Ratio (SNR). We were able to achieve a BER of 10^{-1} with SNR between 5-10 dB and a 0.48 Mbps increase in throughput performance compared to conventional methods. Moreover, IAFIR exhibits substantial improvements in the fairness index, approaching a value of 1 and shows a 4 dB increase in the carrier-to-interference ratio. Its iterative nature enables adaptive filtering, ensuring robust performance across diverse channel conditions. Additionally, the inclusion of a cyclic prefix in IAFIR aids in interference mitigation by introducing a guard interval between symbols, mitigating the effects of multipath fading and ensuring reliable signal transmission. This research not only validates the effectiveness of IAFIR but also opens avenues for exploring its compatibility with various transmit and receiver diversity techniques in multiuser environments. In summary, IAFIR represents a transformative breakthrough in NOMA systems, offering a comprehensive solution to long-standing challenges and laying the groundwork for enhanced wireless communication capabilities in multiuser scenarios.

Acknowledgment

The authors are grateful for the reviewer's valuable comments that improved the manuscript.

Funding Information

The authors have not received any financial support or funding to report.

Author's Contributions

Both authors have equally contributed to this manuscript.

Ethics

The conducted research is not related to either human or animal use.

References

Abd-Alaziz, W., Jebur, B., Fakhrey, H., Mei, Z., & Rabie, K. (2023). A Low-Complexity Coding Scheme for NOMA. *IEEE Systems Journal*, *17*(3), 4464-4473. https://doi.org/10.36227/techrxiv.21631832

Budhiraj, I., Kumar, N., & Tyagi, S. (2022). ISHU: Interference Reduction Scheme for D2D Mobile Groups Using Uplink NOMA. *IEEE Transactions on Mobile Computing*, *21*(9), 3208-3224. https://doi.org/10.1109/tmc.2021.3051670

Chai, J., Feng, N., Ma, M., Li, Z., & Li, S. (2023). NOMA in Flexible Optical Access Network: Principle, Advantage and Challenges. *2023 21st International Conference on Optical Communications and Networks (ICOCN)*, 10236213. https://doi.org/10.1109/icocn59242.2023.10236213

Chauhan, A., & Jaiswal, A. (2024). Multidimensional Signal Space Non-Orthogonal Multiple Access with Imperfect SIC: A Novel SIC Reduction Technique. *IEEE Transactions on Vehicular Technology*, *73*(2), 2374-2389. https://doi.org/10.1109/tvt.2023.3321072

Chen, L., Peizhe, L., Zhenfeng, X., Yefan, W., Haotian, L., Xin, D., & Jiayun, Z. (2021). Research on Power Allocation Algorithm for Maximizing Energy Efficiency in Uplink NOMA System of 5G Smart Grid. *2021 3rd International Conference on Smart Power and Internet Energy Systems (SPIES)*, 9633963. https://doi.org/10.1109/spies52282.2021.9633963

Chitra, S., & Kumaratharan, N. (2015). Intercarrier Interference Reduction in MC-CDMA System through Second Order Duobinary Coded Phase Rotated Conjugate Cancellation Scheme. *PLOS ONE*, *10*(3), e0116326. https://doi.org/10.1371/journal.pone.0116326

Chitra, S., Kumaratharan, N., & Ramesh, S. (2020). A novel subspace method for precise carrier frequency offset estimation in multicarrier modulation scheme under multiuser environment. *International Journal of Communication Systems*, *33*(17), e4608. https://doi.org/10.1002/dac.4608

Chitra, S., Ramesh, S., Vijay, R., Jegan, G., & Lawrence, T. S. (2023). Joint CFO and channel estimation using pilot aided interpolation for high performance MIMO-OFDM. *International Journal of Electronics*, *110*(7), 1355-1372. https://doi.org/10.1080/00207217.2022.2087918

Choi, J. (2018). On Power and Rate Allocation for Coded Uplink NOMA in a Multicarrier System. *IEEE Transactions on Communications*, *66*(6), 2762-2772. https://doi.org/10.1109/tcomm.2018.2807449

CISCO. (2023). *Creating a world of potential*. Cisco 2023 Annual Report. https://www.cisco.com/c/dam/en_us/about/annual-report/cisco-annual-report-2023.pdf

Ghafoor, U., Ali, M., Khan, H. Z., Siddiqui, A. M., & Naeem, M. (2022). NOMA and future 5G & B5G wireless networks: A paradigm. *Journal of Network and Computer Applications*, *204*, 103413. https://doi.org/10.1016/j.jnca.2022.103413

Hama, Y., & Ochiai, H. (2023). Time-Frequency Domain Non-Orthogonal Multiple Access for Power Efficient Communications. *IEEE Transactions on Wireless Communications*, *22*(9), 5711-5724. https://doi.org/10.1109/twc.2023.3235910

He, X., Huang, Z., Wang, H., & Song, R. (2023). Sum Rate Analysis for Massive MIMO-NOMA Uplink System with Group-Level Successive Interference Cancellation. *IEEE Wireless Communications Letters*, *12*(7), 1194-1198. https://doi.org/10.1109/lwc.2023.3266026

Hu, C., Wang, H., Li, C., & Song, R. (2023). Group-based successive interference cancellation for multi-antenna NOMA system with error propagation. *China Communications*, *20*(8), 276-287. https://doi.org/10.23919/jcc.fa.2022-0611.202308

Issa, H., Shehab, M., & Alves, H. (2023). Meta-Learning Based Few Pilots Demodulation and Interference Cancellation for NOMA Uplink. *2023 Joint European Conference on Networks and Communications and 6G Summit (EuCNC 6G Summit)*, 10188320. https://doi.org/10.1109/eucnc/6gsummit58263.2023.10188320

Jehan, A., & Zeeshan, M. (2022). Comparative Performance Analysis of Code-Domain NOMA and Power-Domain NOMA. *2022 16th International Conference on Ubiquitous Information Management and Communication (IMCOM)*, 9721725. https://doi.org/10.1109/imcom53663.2022.9721725

Khan, M. A. A., Kaidi, H. M., Ahmad, N., & Rehman, M. U. (2023). Sum Throughput Maximization Scheme for NOMA-Enabled D2D Groups Using Deep Reinforcement Learning in 5G and Beyond Networks. *IEEE Sensors Journal*, *23*(13), 15046-15057. https://doi.org/10.1109/jsen.2023.3276799

Mai, L., Zhang, Q., & Qin, J. (2021). System Throughput Maximization of Uplink NOMA Random Access Systems. *IEEE Communications Letters*, *25*(11), 3654-3658. https://doi.org/10.1109/lcomm.2021.3107417

Mohsan, S. A. H., Li, Y., Shvetsov, A. V., Varela-Aldás, J., Mostafa, S. M., & Elfikky, A. (2023). A Survey of Deep Learning Based NOMA: State of the Art, Key Aspects, Open Challenges and Future Trends. *Sensors*, *23*(6), 2946. https://doi.org/10.3390/s23062946

Pavithra, S., & Chitra, S. (2023). Review of Non-Orthogonal Multiple Access Schemes and Challenges in Wireless Body Area Network. *2023 3rd International Conference on Advance Computing and Innovative Technologies in Engineering (ICACITE)*, 10182500. https://doi.org/10.1109/icacite57410.2023.10182500

Pischella, M., Chorti, A., & Fijalkow, I. (2020). Performance Analysis of Uplink NOMA-Relevant Strategy Under Statistical Delay QoS Constraints. *IEEE Wireless Communications Letters*, *9*(8), 1323-1326. https://doi.org/10.1109/lwc.2020.2990563

Qin, Z., Yue, X., Liu, Y., Ding, Z., & Nallanathan, A. (2018). User Association and Resource Allocation in Unified NOMA Enabled Heterogeneous Ultra Dense Networks. *IEEE Communications Magazine*, *56*(6), 86-92. https://doi.org/10.1109/mcom.2018.1700497

Rito, B. Y. D., & Li, K. H. (2023). RIS-Assisted NOMA With Interference-Cancellation and Interference-Alignment Scheme. *IEEE Communications Letters*, *27*(3), 1011-1015. https://doi.org/10.1109/lcomm.2023.3235254

Soni, S., Bankar, N. M., Makkar, R., Rawal, D., Sharma, N., & Maradia, K. G. (2023). Opportunistic Interference Alignment for Cognitive MIMO-NOMA Downlink Networks. *2023 2nd Edition of IEEE Delhi Section Flagship Conference (DELCON)*, 10127479. https://doi.org/10.1109/delcon57910.2023.10127479

Srinivasan, S., Dikmese, S., & Renfors, M. (2021). Effects of RF Imperfections on Interference Rejection Combining Based Black-Space Cognitive Radio. *2021 IEEE 93rd Vehicular Technology Conference (VTC2021-Spring)*, 9448895. https://doi.org/10.1109/vtc2021-spring51267.2021.9448895

Tabeshnezhad, A., Swindlehurst, A. L., & Svensson, T. (2023). RIS-Assisted Interference Mitigation for Uplink NOMA. *2023 IEEE Wireless Communications and Networking Conference (WCNC)*, 10119107. https://doi.org/10.1109/wcnc55385.2023.10119107

Zhu, R., Guo, J., Wang, F., Lin, B., & Chen, Y. (2023). Spectrum Efficient Resource Allocation of NOMA Downlink System with MMSE Receiver. *IEEE Access*, *11*, 27414-27425. https://doi.org/10.1109/access.2023.3258451